Atmos. Chem. Phys. Discuss., 15, 25647–25694, 2015
www.atmos-chem-phys-discuss.net/15/25647/2015/
doi:10.5194/acpd-15-25647-2015

Atmospheric Chemistry and Physics Discussions
Open Access

Comparing model and measured ice crystal concentrations in orographic clouds during the INUPIAQ campaign

R. J. Farrington[1], P. J. Connolly[1], G. Lloyd[1], K. N. Bower[1], M. J. Flynn[1], M. W. Gallagher[1], P. R. Field[2,3], C. Dearden[1], and T. W. Choularton[1]

[1]School of Earth, Atmospheric and Environmental Sciences, The University of Manchester, Manchester, UK
[2]Met Office, Exeter, UK
[3]ICAS, University of Leeds, Leeds, UK

Received: 17 July 2015 – Accepted: 30 August 2015 – Published: 21 September 2015

Correspondence to: R. J. Farrington (robert.farrington@manchester.ac.uk) and P. J. Connolly (paul.connolly@manchester.ac.uk)

Published by Copernicus Publications on behalf of the European Geosciences Union.

ACPD
15, 25647–25694, 2015

Abstract

This paper assesses the reasons for high ice number concentrations observed in orographic clouds by comparing in-situ measurements from the Ice NUcleation Process Investigation And Quantification field campaign (INUPIAQ) at Jungfraujoch, Switzerland (3570 m a.s.l.) with the Weather Research and Forecasting model (WRF) simulations over real terrain surrounding Jungfraujoch. During the 2014 winter field campaign, between the 20 January and 28 February, the model simulations regularly underpredicted the observed ice number concentration by $10^3\,L^{-1}$. Previous literature has proposed several processes for the high ice number concentrations in orographic clouds, including an increased ice nuclei (IN) concentration, secondary ice multiplication and the advection of surface ice crystals into orographic clouds. We find that increasing IN concentrations in the model prevents the simulation of the mixed-phase clouds that were witnessed during the INUPIAQ campaign at Jungfraujoch. Additionally, the inclusion of secondary ice production upwind of Jungfraujoch into the WRF simulations cannot consistently produce enough ice splinters to match the observed concentrations. A surface flux of hoar crystals was included in the WRF model, which simulated ice concentrations comparable to the measured ice number concentrations, without depleting the liquid water content (LWC) simulated in the model. Our simulations therefore suggest that high ice concentrations observed in mixed-phase clouds at Jungfraujoch are caused by a flux of surface hoar crystals into the orographic clouds.

1 Introduction

Orographic clouds, and the precipitation they produce, play a key role in the relationship between the atmosphere and the land surface (Roe, 2005). The formation and development of each orographic cloud event varies considerably. Variations in the large-scale flow over the orography, the size and shape of the orography, convection, turbulence and cloud microphysics all influence the lifetime and extent of orographic clouds, as well as the intensity of precipitation they produce (Rotunno and Houze, 2007). Understanding these variations in orographic clouds is important as the intensity and extent of a wide-range of geophysical hazards are heavily influenced by precipitation (Conway and Raymond, 1993; Galewsky and Sobel, 2005).

The influence of aerosols on the cloud microphysical processes is thought to be important in understanding the variability of orographic clouds and precipitation. Aerosols interact with clouds by acting as cloud condensation nuclei (CCN) which water vapour condenses on to, or ice nuclei (IN). The differing efficiencies, compositions and concentrations of both CCN and IN in the atmosphere influence the lifetime and precipitation efficiency of clouds (Twomey, 1974; Albrecht, 1989; Lohmann and Feichter, 2005).

In particular, the role of aerosols in the production of ice in the atmosphere is poorly understood. Ice can nucleate in the atmosphere without the presence of IN at temperatures below $-38\,^{\circ}$C via homogeneous nucleation (Koop et al., 2000). However, it is thought that for temperatures greater than $-38\,^{\circ}$C most ice nucleation in orographic clouds takes place heterogeneously on IN via different freezing mechanisms: deposition, condensation freezing, immersion freezing and contact freezing (Vali, 1985). Above $-38\,^{\circ}$C, the presence of supercooled liquid water has consistently been found to be a requirement of significant heterogeneous nucleation (Westbrook and Illingworth, 2011, 2013; de Boer et al., 2011), causing the immersion, contact and condensation freezing modes to dominate ice production at these temperatures (de Boer et al., 2011; Field et al., 2012).

Despite much uncertainty existing over the concentrations and distributions of IN in the atmosphere (Boucher et al., 2013), particular aerosol particle types have been proposed to nucleate ice. Several studies suggest that mineral dust nucleates ice in the atmosphere (e.g. DeMott et al., 2003; Cziczo et al., 2013), although the temperature threshold below which dust aerosols nucleates ice varies significantly between studies, with some suggesting dust could act as IN at temperatures as high as $-5\,^{\circ}$C (Sassen et al., 2003), whilst others found dust IN to be inactive above $-20\,^{\circ}$C (Ansmann et al., 2008). Laboratory measurements of ice nucleation on desert dust aerosols have linked

ACPD
15, 25647–25694, 2015

the varying nucleation threshold temperatures to the mineral composition of the dust particles (Connolly et al., 2009; Murray et al., 2011; Broadley et al., 2012; Niemand et al., 2012; Atkinson et al., 2013; Emersic et al., 2015). Generally the literature has suggested that mineral dust is unlikely to act as an IN at temperatures as high as −5 °C, which has led to ongoing research into whether other aerosol components can nucleate ice at higher temperatures than mineral dust. Biological aerosols such as bacteria or pollen have been suggested as potentially being suitable to nucleate ice heterogeneously (Möhler et al., 2007), which has been supported by in-situ observations (Prenni et al., 2009; Pratt et al., 2009). However, despite some laboratory experiments suggesting that certain bacteria nucleate ice at temperatures greater than −10 °C in the atmosphere (Hoose and Möhler, 2012), there remains an uncertainty in the role of biological aerosols in ice nucleation at higher temperatures.

IN concentrations alone are not enough to explain ice number concentrations witnessed in some clouds. Ice concentrations in the atmosphere can also be increased by ice multiplication processes. The Hallett–Mossop process (Hallett and Mossop, 1974; Mossop and Hallett, 1974), which produces ice splinters during the riming of ice particles, has been suggested as a dominant ice multiplication process between temperatures of −3 and −8 °C. Mossop and Hallett (1974) indicated that one splinter is produced for every 160 droplets accreted to the ice crystal, providing the droplets are greater than 20 µm in diameter, and suggested that several rime-splinter cycles could increase ice number concentrations by as much as five orders of magnitude. Several examples have been presented in the literature of the Hallett–Mossop process explaining differing IN and ice number concentrations (Harris-Hobbs and Cooper, 1987; Hogan et al., 2002; Huang et al., 2008; Crosier et al., 2011; Lloyd et al., 2014). However, the process is limited to specific regions, which are within the required temperature range, have large concentrations of supercooled liquid droplets, and in clouds with long lifetimes (> 25 min) and weak updrafts (Mason, 1996). More recently Lawson et al. (2015) has shown fragmentation of freezing drops can also act as a secondary ice multiplica-

ACPD
15, 25647–25694, 2015

tion mechanism in the absence of the Hallett–Mossop process, particularly in cumuli with active warm rain processes.

Despite considerable improvement in the understanding of ice production processes in the atmosphere, much confusion remains in understanding the sources of ice measured in orographic clouds. Several studies have found significantly high ice number concentrations at mountain sites when compared to aircraft observations. Rogers and Vali (1987) frequently found ice concentrations close to the surface of Elk Mountain of three orders of magnitude higher than concentrations measured by aircraft 1 km above the mountain. The increased concentrations could not be explained by Hallett–Mossop ice multiplication, leading them to suggest the possibility of surface ice or snow crystals being blown into the cloud. Vali et al. (2012) proposed that ground-layer snow clouds, which are formed by snow blown up from the surface and growing in an ice supersaturated environment, were responsible for the increased ice number concentrations. Targino et al. (2009) found two cases of high ice concentrations at Jungfraujoch in Switzerland, and suggested that the high ice concentrations were unlikely to be caused by mineral dust IN, as no significant increase in dust aerosol concentrations was observed. They suggested that polluted aerosol, such as black carbon, acted as IN and increased the ice concentration close to the surface. During the Ice NUcleation Process Investigation And Quantification field campaign (INUPIAQ) undertaken during the winter of 2013 and 2014, Lloyd et al. (2015) found ice number concentrations of over $\sim 2000\,\mathrm{L}^{-1}$ at $-15\,^{\circ}$C. By using measured aerosol concentrations in the parameterisation of DeMott et al. (2010), they predicted IN concentrations which were as much as 3 orders of magnitude smaller than the ice number concentration. Whilst their findings suggested blowing snow contributed to the ice number concentrations, they found the effect could not fully explain the high ice concentration events where concentrations were $> 100\,\mathrm{L}^{-1}$. However, they suggested that a flux of particles from the surface, such as surface hoar crystals, could provide enough ice crystals to match the high ice number concentrations witnessed in their field campaign.

ACPD
15, 25647–25694, 2015

With aerosol and cloud particle measurements limited over mountainous regions, research into orographic clouds has been driven by the modelling community. However, the complexity of the atmospheric dynamics, cloud microphysics and terrain has often led to a restricted approach in investigating orographic clouds (Kunz and Kottmeier, 2006; Barstad et al., 2007; Cannon et al., 2014). Whilst 3-D atmospheric models provide a more accurate representation of the complex airflow which mountainous terrain generates, the computational expense has generally limited studies of aerosol-cloud interactions in orographic clouds to 2-D simulations (Lynn et al., 2007; Zubler et al., 2011) or idealised terrain (Xiao et al., 2014). Recently, Muhlbauer and Lohmann (2009) performed 3-D simulations over idealised orography to investigate the influence of aerosol perturbations of dust and black carbon on the cloud microphysical processes in mixed-phase clouds. The simulations were run using a two-moment mesoscale model with coupled aerosol and cloud microphysics and 3-D idealised orography. Muhlbauer and Lohmann (2009) suggested that aerosols are critical in initiating ice in mixed-phase orographic clouds. However the strength of their conclusions are limited to the idealized terrain used in the model, and for the specific aerosol data from 2009.

By drawing on previous research into orographic clouds using modelling, this paper aims to assess the reasons for high ice number concentrations at mountain sites by comparing the in-situ measurements of Lloyd et al. (2015) from the INUPIAQ campaign with simulations over real terrain from the Weather Research and Forecasting model (WRF). In Sect. 2, we outline the characteristics of the field site and the instrumentation used to measure cloud microphysical properties, before providing a description of the implementation of the WRF model. In Sect. 3, we provide validation of the model using meteorological data from stations throughout the model domain. The in-situ ice number concentrations are then compared with the WRF model in Sect. 4, before analysing the processes proposed in previous literature for increasing ice concentrations in orographic clouds using further WRF simulations. Finally, in Sect. 5, we evaluate the suggested processes that cause high ice concentrations in orographic clouds, and draw conclusions from our results.

ACPD
15, 25647–25694, 2015

2 Methodology

2.1 Jungfraujoch

Cloud particle number concentrations and size distributions were measured at the Jungfraujoch high-alpine research station, located in Bernese Alps in Switzerland. Jungfraujoch is an ideal location to measure microphysical properties of clouds, as the altitude of the site (3570 m a.s.l.) allows measurements to be within cloud 37 % of the time (Baltensperger et al., 1998). The site is only accessible by electric train, which limits the influence of local anthropogenic emissions on measurements taken at Jungfraujoch (Baltensperger et al., 1997). The site has regularly been used for cloud and aerosol research by groups from the Paul Scherrer Insistute, Karlsruhe Institute of Technology, University of Manchester and other institutions (e.g., Baltensperger et al., 1997, 1998; Verheggen et al., 2007; Choularton et al., 2008; Targino et al., 2009; Lloyd et al., 2015).

2.2 Instrumentation at Jungfraujoch

Several cloud physics probes using a variety of measurement techniques were used for measuring cloud particle number concentrations and size distributions during the campaign. The probes were mounted on the roof terrace of the Sphinx laboratory on a rotating wing attached to a ∼ 3 m high tall mast, which was automatically rotated and tilted to face into the wind based on the measured wind direction to minimize inlet sampling issues.

Ice concentrations were primarily measured using an aspirated Three-View Cloud Particle Imager (3V-CPI) by Stratton Park Engineering Inc (SPEC). This probe is a combination of two previously separately packaged instruments: the Two-Dimensional Stereo Hydrometeor Spectrometer (2D-S) and a Cloud Particle Imager (CPI). The 2D-S produces shadow imagery of particles by illuminating them onto 128 photodiode arrays, with a pixel resolution of 10 µm, as they pass through the cross-section of two diode laser beams (Lawson et al., 2006). The arrays allow images in 2 dimensions of particles in the cross-section of both laser beams, in addition to providing number concentrations and size distributions of particles in the size range of 10–1260 µm. The raw data provided was then processed using the Optical Array Shadow Imaging Software (OASIS) to segregate ice and droplets based on their shape, and to remove particles that had shattered on the 2D-S from the dataset (Crosier et al., 2011). Further details of the 2D-S analysis are provided by Lloyd et al. (2015). When particle images are recorded on both arrays of photodiodes on the 2D-S, the CPI probe is activated. The CPI images the particle motion using a 20 ns pulsed laser, casting an image of the particle onto a 1024 by 1024 array. The CPI has a pixel resolution of 2.3 µm and thus has a size range of between 10–2000 µm (Lawson et al., 2001). CPI produces clear images of crystals and processing of the raw data enables the habit of the crystals to be estimated. However, corrections must be made to include out-of-focus particles and for particles below 50 µm, as the sample volume has a size dependency for small particles (see Connolly et al., 2007).

Droplet concentrations and liquid water content (LWC) were measured by the Forward Scattering Spectrometer Probe (FSSP), and the Cloud Droplet Probe (CDP) which use the forward scattering of light from a laser to count and size water droplets of diameters of between 2 and 50 µm (Lance et al., 2010). Meteorological conditions were recorded with a Vaisala probe, which measured temperature and relative humidity, and a Metek sonic anemometer, which measured the temperature, wind speed and direction. Additionally, meteorological data was available from the MeteoSwiss observation station at Jungfraujoch for comparison. Further details of the instrumentation can be found in Lloyd et al. (2015).

2.3 Model setup

To compare with the measurements made by cloud microphysics probes at Jungfraujoch, version 3.6 of the WRF model was used (Skamarock et al., 2008). A single model domain was set up surrounding Jungfraujoch, with a horizontal resolution of 1 km, covering 149 grid points in the north-south direction and 99 grid points in the east-west direction. The higher spatial resolution was required as the real orography is more complicated than the idealised topography used by Muhlbauer and Lohmann (2009). 99 vertical levels were used, which follow the terrain as “sigma” levels, providing a level spacing of between 58 and 68 m close to the terrain surface, and between 165 and 220 m at the model top, which was situated at ~ 20 km. A time-step of 3 s was used, to satisfy the Courant–Friedrichs–Lewy (CFL) stability criterion, as the complex orography surrounding Jungfraujoch can cause CFL violations.

The orography in the model is interpolated from surface data with a resolution of $2'$, with the height of Jungfraujoch in the model being 3330 m a.s.l. The resolution of $2'$ was used as the steep gradients present in the $30''$ orographic data cause CFL stability problems, which prevent the model simulation from running over the Jungfrau region for the duration of the field campaign. The model was run using operational analysis data from the European Centre for Medium-range Weather Forecasting to initialise the model and provide boundary conditions at the edge of the domain, which were updated every 6 h. The model simulations were found to have a spin-up time of 40 h using the vertical wind field that was output from the simulation.

To model the cloud microphysics, the Morrison two-moment scheme was used, which is described in Morrison et al. (2005, 2009). The number of ice crystals per litre produced from heterogeneous freezing, N_i, is defined using the Cooper equation (Cooper, 1986; Rasmussen et al., 2002):

$$N_i = 0.005 \exp\left[0.304\,(T_0 - T)\right] \tag{1}$$

where $T_0 = 273.15$ K and T is the temperature in K. The equation is based on in-situ measurements of heterogeneous ice nucleation by deposition and condensation freezing. At $T = 258.15$ K (−15 °C), the parameterisation predicts ice concentrations of 0.4779 L^{-1}. Chou et al. (2011) measured IN concentrations at Jungfraujoch of approximately 10 L^{-1} below water saturation using a portable ice nucleation chamber at −29 °C, whilst Conen et al. (2015) measured concentrations of 0.01 L^{-1} at −10 °C.

ACPD
15, 25647–25694, 2015

As the Cooper parameterisation predicts IN concentrations between these values, the parameterisation can be used to assess the ice concentration at Jungfraujoch. The conditions which the parameterisation is used were adapted for the Morrison Scheme from Thompson et al. (2004), and hence is active either when the saturation ratio with respect to ice is greater than 1.08 or when the model is saturated with respect to water and the temperature of the model is below $-8\,^{\circ}$C.

The short-wave and long-wave radiation are parametrised in the model using the Goddard scheme (Chou and Suarez, 1999). No cumulus parameterisations were used, as the resolution of the model should provide sufficient detail to resolve clouds at grid-scale.

Several WRF simulations were run as part of our investigation, and these are summarised in Table 1. Each simulation was run for the time period of the INUPIAQ campaign, between the 20 January 2014 00:00 Z and 28 February 2014 00:00 Z, and completed in a single, continuous model simulation with no re-initialised simulations used in our research. The initial WRF simulation for INUPIAQ formed a control simulation to assess the validity of the model, as well as allowing a basis for comparison with simulations adjusted to include additional microphysical processes.

3 Model validation

To assess the validity of the model, the WRF control simulation was compared with observed meteorological data from a number of MeteoSwiss observation stations throughout the domain, listed in Table 2. Each site provided data for wind speed, wind direction, temperature and relative humidity, which is compared with the output from the control simulation in Figs. 1–4.

Figures 1–4 show that the meteorological data compares favourably with the meteorological variables simulated in the WRF control simulation. At Jungfraujoch, the model closely follows the observed temperature throughout the campaign at all times where observed data was available. At other sites, the temperature is less accurate, with periods during the campaign where observations at Titlis showed significantly lower temperatures and relative humidities, and higher wind speeds, than the values determined from the WRF simulation. The differences between the simulation and observations at Titlis relate to the close proximity of the station to the edge of the domain, where the model is more sensitive to the boundary conditions, causing the discrepancy between the control simulation and the meteorological observations. However, as Jungfraujoch is at the centre of the model domain, it is not sensitive to boundary conditions. Also, the resolution of the orography causes the height of the sites in the model to be reduced. The height at Titlis in the model is 2234 m a.s.l., much lower than the actual height (3040 m a.s.l.) of the site. As a result, the temperature in the model will be warmer as the location of Titlis in the model is lower in altitude. In contrast, the difference in height between the model and reality is much smaller at Jungfraujoch (~ 280 m), so the difference in temperature is considerably less. Hence the MeteoSwiss data shows that the model provides a good representation of the atmospheric conditions over Jungfraujoch for our research.

4 Comparison and explanations for differences between modelled and observed ice number concentrations

For the duration of the campaign, the ice number concentrations recorded using the 2D-S were compared with ice number concentrations simulated in the WRF control simulation (see red and blue lines in Fig. 5a). The control simulation regularly produced around 10^3 fewer ice crystals than measured by the 2D-S at Jungfraujoch, similar to the discrepancies found in the literature between ice concentrations measured at mountain sites and on aircraft (Rogers and Vali, 1987), and between ice concentrations and predicted IN concentrations (Lloyd et al., 2015). We will now examine the cause of the discrepancy between the ice number concentrations simulated in WRF and the concentrations measured at Jungfraujoch.

ACPD
15, 25647–25694, 2015

Comparing Model and Measured Ice Crystal Concentrations

R. J. Farrington et al.

Title Page
Abstract Introduction
Conclusions References
Tables Figures
◂ ▸
Back Close
Full Screen / Esc
Printer-friendly Version
Interactive Discussion

4.1 Sensitivity of simulation to IN concentration

We first examine if the difference between modelled and measured ice concentrations is explained by additional IN in the model. As touched upon in Sect. 2.3, measurements from previous field campaigns at Jungfraujoch have suggested varying IN concentrations of between 10 and 0.01 L^{-1} (Chou et al., 2011; Conen et al., 2015). Whilst the previously measured IN concentrations have varied, they are still considerably lower than the ice number concentrations measured at Jungfraujoch (Lloyd et al., 2015). Hence there is a possiblity that other aerosols are nucleating ice which are not sampled by the instruments measuring IN concentrations at Jungfraujoch, as proposed by Targino et al. (2009).

To test this hypothesis, two further WRF simulations were run with increased IN concentrations. The IN concentrations were increased by multiplying the number of IN per litre from the Cooper equation (Cooper, 1986) by a constant value. In the two simulations, IN-1 and IN-3, the IN concentrations were multiplied by 10 and 10^3 respectively. The ice number concentrations simulated at Jungfraujoch in the control, IN-1 and IN-3 WRF simulations are compared with the 2D-S concentrations in Fig. 5a.

A better comparison between the model ice number concentrations and the 2D-S concentrations is found when the number of IN is multiplied by 10^3. Taken in isolation, the ice number concentration simulated in the IN-3 simulation suggests that the Cooper equation used in the Morrison scheme significantly underestimates the IN concentrations in orographic clouds and that additional IN are present in a mountainous environment.

However, increasing the IN concentration in the Morrison scheme generally causes the LWC in the simulation to decrease (see Fig. 5b). When freezing occurs in mixed phase clouds, ice crystals grow at the expense of liquid droplets by the Bergeron–Findesen process. The greater IN concentration in the model increases the number of small ice crystals produced at the onset of freezing. Figure 5b indicates that multiplying the IN concentration by 10^3 generally causes the LWC to decrease to zero, with

ACPD
15, 25647–25694, 2015

liquid water absent at Jungfraujoch for most of the IN-3 simulation. However, measurements from several liquid and ice cloud probes during the field campaign, as well as measurements made in previous field campaigns at Jungfraujoch, suggest liquid water is present even when large ice number concentrations are measured (Targino et al., 2009; Lloyd et al., 2015).

The IN-3 WRF simulation implies that concentrations similar to the measured ice number concentrations are not possible in mixed-phase clouds, which is in contrast to the measurements made at Jungfraujoch. However, as multiple ice and liquid probes from different field campaigns agree on the presence of both high ice concentrations and liquid water at Jungfraujoch (Choularton et al., 2008; Targino et al., 2009; Lloyd et al., 2015), it is unlikely that increasing IN in the model is the correct explanation for the observed ice number concentrations at Jungfraujoch.

Validation of mixed phase cloud at Jungfraujoch

To confirm that mixed-phase clouds are possible at Jungfraujoch with the both the measured and modelled ice number concentrations, we used the conditions for the existence of mixed-phase clouds derived by Korolev and Mazin (2003). In their paper, Korolev and Mazin (2003) provide an updraft speed threshold, above which mixed-phase conditions in a cloud can be maintained by the updraft speed. The threshold is based on the assumptions of a parcel model, and that a cloud must be water saturated for droplets to exist in clouds. The threshold updraft speed is defined by

$$u_{z,t} = \frac{b_i^* N_i \bar{r}_i}{a_0} \tag{2}$$

where N_i is the number concentration of ice crystals, $\bar{r}_i$ is the mean radius of ice crystals, and a_0 and b_i^* are thermodynamic variables dependant on the pressure and temperature of the parcel, as defined in Korolev and Mazin (2003).

The threshold updraft speed was calculated for both the measured and modelled ice concentration. For the measured ice concentrations, the term $N_i \bar{r}_i$ was calculated

ACPD
15, 25647–25694, 2015

using the 2D-S size distribution, with measurements of temperature and pressure from Jungfraujoch also used to calculate $u_{z,t}$. The updraft speeds measured by the sonic anemometer at Jungfraujoch were then compared to $u_{z,t}$. For the modelled ice concentrations, the term $N_i \bar{r}_i$ was calculated from the first moment of the ice, snow and graupel size distributions from the control and IN-3 WRF simulations, using the gamma size distribution parameters from the Morrison scheme (see Appendix of Morrison et al., 2005). The snow and graupel size distributions are included in the calculation, as the growth of both snow and graupel also depletes the LWC by the Bergeron–Findeisen process. Additionally, the simulated temperature and pressure from each simulation were used in the calculation of $u_{z,t i}$, which was then compared with the simulated updraft speeds from the two simulations.

For the majority of the campaign, the updraft speed measured at Jungfraujoch was greater than the threshold updraft velocity for mixed-phase cloud conditions (Fig. 6a), which is consistent with the coexistence of liquid water and ice crystals witnessed at Jungfraujoch. Assuming that the atmosphere is saturated with respect to liquid, the updraft threshold reinforces the measurements in suggesting that droplets and ice can coexist in clouds at Jungfraujoch, as indicated by the 2D-S and CDP measurements in Fig. 5a and b.

For the control WRF simulation, Fig. 6b shows the low ice concentrations significantly reduce $u_{z,t}$, such that the threshold is approximately two orders of magnitude smaller than the updrafts simulated at Jungfraujoch. When the IN concentrations in the WRF model are increased, more ice crystals are produced, which is caused by the vapour deposition onto the additional IN. The vapour deposition results in a reduction of the saturation ratio in the model. To maintain a saturation ratio which is greater than liquid saturation, a greater updraft speed is required. Hence increasing the IN concentration in WRF increases the updraft speed threshold for the existence of mixed-phase clouds.

Figure 6b indicates that, when the IN concentrations are increased, the updraft speed threshold increases significantly to values close to u_z throughout the field campaign. During some periods, the simulated updraft speed is lower than the updraft speed

ACPD
15, 25647–25694, 2015

threshold from the IN-3 simulation. During other periods, there is no updraft present, which would prevent mixed-phase conditions from being sustained. As the updraft speed is either lower than the threshold during these periods, or not present at all, the Korolev and Mazin analysis predicts that mixed-phase clouds will not occur during these periods. The analysis supports the findings of the IN-3 simulation indicated in Fig. 5a and b.

The absence of the observed mixed-phase clouds in the IN-3 simulation implies that increasing the IN concentration alone can not explain the measured ice number concentrations at Jungfraujoch. Results from our modelling suggest additional microphysical processes are important in the production of ice in orographic mixed-phase clouds.

4.2 Hallett–Mossop process upwind of Jungfraujoch

Ice multiplication processes such as the Hallett–Mossop process (Hallett and Mossop, 1974) have been suggested as an important mechanism in the production of ice crystals in mixed-phase clouds. Rogers and Vali (1987) suggested in their study at Elk Mountain that the Hallett–Mossop is not responsible for the increased ice number concentrations as the droplet sizes are not sufficiently large enough to cause splinter production. In addition they suggested that temperatures witnessed at Elk Mountain are outside the Hallett–Mossop temperature range of -3 to $-8\,^{\circ}$C. During the INUPIAQ campaign, the temperatures observed at Jungfraujoch were generally colder than $-8\,^{\circ}$C, ruling out secondary ice production at the site via the Hallett–Mossop process (Lloyd et al., 2015). However, Targino et al. (2009) suggested that as Jungfraujoch is generally above cloud base, the Hallett–Mossop process could occur below Jungfraujoch at higher temperatures, and that splinters could be lifted from the cloud base to increase ice number concentrations at the summit. For secondary ice production to occur at cloud base, supercooled liquid water and ice crystals must both be present. In addition, the temperature at cloud base must be within the Hallett–Mossop tempera-

Discussion Paper | Discussion Paper | Discussion Paper | Discussion Paper |

ACPD
15, 25647–25694, 2015

Comparing Model and Measured Ice Crystal Concentrations

R. J. Farrington et al.

ture range, and a strong updraft must be present to advect the newly produced splinters towards Jungfraujoch.

To establish if splinters were transported to Jungfraujoch from cloud base, back trajectories were calculated using the WRF control simulation output. By assuming the wind field $-u_{ijk}$ at the initial output time was constant along the back trajectory, the back trajectories were calculated using

$$\Delta x_{ijk} = -u_{ijk}\Delta t \tag{3}$$

where $\Delta t = 30$ is the time step in seconds. At each point along the trajectories, the WRF output fields were interpolated from nearest WRF output variables to the point. Using the LWC q_l and ice number concentration n_{ice}, the production rate of splinters formed by the Hallett–Mossop process was calculated using

$$\frac{\mathrm{d}n_{i,\mathrm{hm}}}{\mathrm{d}t} = q_l V_\mathrm{f} A \eta n_{\mathrm{ice}} \tag{4}$$

with V_f denoting the fall speed of the ice particle, A denoting the area swept out by the ice crystal and η the number of splinters produced per µg of rime. η is defined as 350×10^6 splinters kg^{-1} following Mossop and Hallett (1974), whilst the ice crystals were assumed to be spherical with diameters of 500 µm, and falling at $2\,\mathrm{m\,s}^{-1}$. As the model resolution is finite we define the temperature thresholds within which splinters are produced, conservatively using a slightly wider temperature range than Hallett and Mossop (1974), with the production rate set to 0 if the temperature was greater than $-2\,^{\circ}\mathrm{C}$ or less than $-10\,^{\circ}\mathrm{C}$. The extended range was to prevent the splinter concentration being underestimated due to any differences between the constant temperature field in the model and the real temperature. The cumulative number of splinters produced along each back trajectory was then calculated, to provide a maximum number of splinters that could be produced along the back trajectory. The calculation of the total concentration of ice splinters along the back trajectory assumes that every ice splinter produced along the back trajectory is transported to Jungfraujoch and measured as

ACPD
15, 25647–25694, 2015

an ice crystal, which is unlikely as the ice crystals would be reduced along the back trajectory by sedimentation or collisions with sedimenting particles.

The total number concentration of splinters produced along the back trajectory was added to the ice number concentration at Jungfraujoch and is compared with the ice number concentrations produced by the WRF control run and the 2D-S in Fig. 7. When including the splinters calculated using Eq. (4), the ice number concentration from the WRF control simulation increases significantly during certain periods of the campaign, as indicated by the grey shaded areas in Fig. 7. For example on 1 February, the addition of splinters increases the WRF ice number concentration to within a factor of 10 of the 2D-S ice number concentration at Jungfraujoch. Figure 8 shows the back trajectory from 1 February 2014 at 19:00 Z, plotted following the direction of the wind, which was south-easterly. The high number of splinters calculated along the back trajectory is due to the constant presence of liquid water and ice crystals, in addition to the initial presence of a suitable temperature for splinter production. The simulation of splinters stops when the temperature falls below $-10\,^{\circ}$C after 20 min, producing a significantly larger concentration of ice splinters than simulated at Jungfraujoch in the control simulation. The conditions along the back trajectory suggest that during this case study the WRF model underpredicts the concentration of ice crystals produced by the Hallett–Mossop process quite considerably. Viewing the case in isolation, the inclusion of splinters produced at cloud base in the model would allow a better representation of the ice concentrations observed at Jungfraujoch.

However, as indicated in Fig. 7 the case on the 1 February is not representative of the whole campaign, with only small concentrations of splinters simulated upwind of Jungfraujoch throughout most of the campaign. Figure 9 illustrates that on 26 January, where the observed and modelled ice number concentration differ by 3 orders of magnitude, no splinters are simulated. The absence of secondary ice along the back trajectory is a response to the temperature remaining below $-10\,^{\circ}$C throughout the ascent of the air towards Jungfraujoch, causing no splinters to be produced despite the presence of both supercooled water and ice crystals. As a result, there is no increase in ice crys-

ACPD
15, 25647–25694, 2015

tal concentration at Jungfraujoch for the 26 January case. Hence, the Hallett–Mossop process occurring below cloud base is not the main reason for the large discrepancy between the measured and modelled ice number concentration during this period.

However, during certain periods splinter production may contribute to the difference between the modelled and measured ice number concentrations. Also, the influence of secondary ice production on the ice concentration in mountainous regions may differ due to seasonal or spatial variations. Secondary ice production may significantly enhance ice number concentrations in regions at different altitudes or at different times of the year, if the temperatures in these regions are within the Hallett-Mossop temperature regime more frequently than witnessed at Jungfraujoch.

4.3 Inclusion of snow concentration in ice concentration

The ice number concentration simulated in WRF may be reduced by the misrepresentation of some ice crystals as snow crystals. Ice is converted to snow in the Morrison scheme when ice size distributions grow by vapour diffusion to sizes greater than a threshold mean diameter. The Morrison scheme uses a threshold mean diameter of 125 µm following Harrington et al. (1995). However, Schmitt and Heymsfield (2014) implied that the threshold diameter can vary significantly in real clouds, suggesting threshold diameters of 150 and 250 µm for two separate case studies. Raising the threshold diameter for autoconversion in the microphysics scheme may provide a simulated ice number concentration which is more representative of the 2D-S measurements at Jungfraujoch.

To assess whether the discrepancy between the measured and modelled ice number concentrations is caused by ice being incorrectly converted to snow, the frozen concentration was calculated by adding the modelled snow and ice number concentrations together. Whilst the snow number concentration will include falling snow in addition to large ice, this is only significant if the frozen concentration is greater than the measured ice number concentration.

The increase in ice number concentration with the addition of snow is not significant enough to match the ice number concentrations observed at Jungfraujoch. Figure 10 suggests the number of snow crystals is small compared to the difference between the modelled and observed ice number concentrations. The inclusion of snow into the ice number concentrations fails to increase the concentrations by the three orders of magnitude required to match the observed concentrations.

4.4 Surface crystal flux

After careful analysis, Lloyd et al. (2015) suggested that whilst blowing snow influenced ice number concentrations periodically, the effect provided only a minor contribution to the ice number concentration at Jungfraujoch. However, they also suggested that a surface ice generation mechanism was potentially the source of the high ice number concentrations witnessed at Jungfraujoch. Along with Rogers and Vali (1987), they speculated that it was possible for surface hoar crystals growing on the surface of the mountain to be blown by surface winds into the atmosphere and influence the ice number concentration. Surface hoar or hoarfrost forms by deposition of water vapour onto the snow surface in supersaturated air at temperatures below 0 °C (Na and Webb, 2003; Polkowska et al., 2009). Wind also has a significant effect on surface hoar development, with ideal wind speeds for formation between 1–2 $\mathrm{m\,s^{-1}}$ (Hachikubo and Akitaya, 1997). Stossel et al. (2010) discovered that surface hoar formation occurs during clear nights with humid air, and can survive throughout the day. Previous research has mostly been motivated by understanding avalanche formation, with research focused on the formation (Colbeck, 1988; Hachikubo and Akitaya, 1997; Na and Webb, 2003) and spatial variability of the phenomena (Helbig and Van Herwijnen, 2012; Shea and Jamieson, 2010; Galek et al., 2015). The research into atmospheric impacts of surface hoar have been limited.

However, the atmospheric influence of frost flowers, a similar phenomena to surface hoar, is the subject of much research. Frost flowers are highly saline crystals which form on freshly formed sea ice that is significantly warmer than the atmosphere above

(Perovich and Richter-Menge, 1994; Style and Worster, 2009). Similarly to surface hoar, they require the presence of supersaturated air with respect to ice above the surface (Rankin et al., 2002), and grow by vapour deposition (Domine et al., 2005). Atmospheric scientists have shown particular interest in the role of frost flowers in the production of sea salt aerosol in the atmosphere (Rankin and Wolff, 2003; Alvarez-Aviles et al., 2008). Xu et al. (2013) provided an observation-based parameterisation of the atmospheric flux of aerosol from frost flowers. The parameterisation has an exponential dependency on wind speed, and was included in the WRF-Chem model. Xu et al. (2013) found the inclusion of frost flowers in the model enabled a better agreement between modelled and measured sea salt aerosol concentrations. Whilst the flux is of sea-salt aerosol, the flux equation does not require the definition of either the aerosol concentration or the frost flower density, and essentially provides a flux which is only dependant on wind-speed. Feick et al. (2007) suggested that the most important influence on surface hoar destruction is wind, implying that the crystals on the surface are removed by the wind blowing the crystals into the atmosphere. As the aerosol flux derived by Xu et al. (2013) and the removal of hoar crystals from the surface are both strongly dependent on wind, the flux can be used to model hoar crystals being blown from the surface. Hence, an adaptation of the aerosol flux is suitable to provide an initial assessment on the influence of surface hoar on the ice number concentrations in orographic clouds.

We adapted the aerosol flux from Xu et al. (2013) for inclusion in our simulations to assess if the discrepancy between modelled and measured ice number concentrations can be found. The surface ice crystal flux ϕ was calculated using

$$\phi = e^{0.24u_\mathrm{h}-0.84} \quad (5)$$

where u_h is the horizontal wind speed. The surface crystal flux was applied to the first level of the model, assuming surface hoar crystals sizes of 10 µm. The flux acts everywhere where the air temperature in the first level of the model is less than 0 °C

ACPD
15, 25647–25694, 2015

and the air is supersaturated with respect to ice, with no dependence on diurnal effects or variations in surface snow cover.

Two WRF simulations were run including the surface crystal flux. Firstly, Surf-6, which assumed the flux magnitude of $10^6\,m^{-2}\,s^{-1}$ following Geever et al. (2005) and Xu et al. (2013). The flux magnitude assumes in the Surf-6 simulation assumes that the number of surface hoar crystals blown into the atmosphere is equal to the number of frost flowers in Xu et al. (2013). The ice number concentration from the Surf-6 simulations are compared with the 2D-S ice number concentration in Fig. 11a. The Surf-6 provides a good agreement with the 2D-S, although with concentrations higher in the model than measured at Jungfraujoch. The 2D-S and the Surf-6 WRF simulation generally differs by approximately a factor of 100 throughout the campaign. The increase in concentration is unsurprising, as the flux is adapted from an equation based on aerosol concentrations emitted from frost flowers. As the surface crystal flux is an ice concentration, the magnitude of the flux is likely to be smaller than the magnitude used by Xu et al. (2013), which was for an aerosol concentration.

As the surface crystal flux is high, a large number of small ice crystals are ejected from the surface in the model. These crystals grow rapidly by vapour deposition in ice supersaturated conditions. In order to continue to grow by vapour deposition, the ice crystals scavenge vapour from any droplets present, and deplete the liquid water from the model by the Bergeron–Findeisen process. As indicated in Fig. 11b, the LWC in the Surf-6 simulation is scavenged by the ice number concentration, and does not agree with LWC measured by the CDP at Jungfraujoch. The large ice number concentration blown into the atmosphere from the surface rapidly depletes the liquid water at Jungfraujoch in the model, suggesting the magnitude of the flux is unrealistic. Hence, the magnitude of the flux would need to be reduced to better represent the ice number concentration at Jungfraujoch, and to prevent liquid water from being depleted from the atmosphere to agree with the measurements taken at Jungfraujoch.

As the Surf-6 simulation overestimated the ice number concentration and underestimated the LWC, a second simulation, Surf-3, was run with the flux magnitude reduced

ACPD
15, 25647–25694, 2015

to $10^3\ m^{-2}\ s^{-1}$. Figure 11a indicates that the Surf-3 provides much better agreement with the ice number concentration measured at Jungfraujoch throughout the campaign. In addition, Fig. 11b shows the LWC simulated in Surf-3 also compares much better with the CDP than Surf-6, with the differences between the model and measurements no greater than a factor of 3, and for the most part of the campaign within a factor of 2.

Figures 12 and 13 show the ice number concentration and LWC from the Surf-3 simulation during a period where both ice and liquid are present at Jungfraujoch. Figure 12 indicate the ice concentration is heavily increased by the surface ice concentration, and that the surface ice is not carried from the surface high into the atmosphere. The high surface concentrations supports the findings of Rogers and Vali (1987) that ice concentrations aloft were much lower than at the surface. The LWC in Fig. 13 is also indicated to be a strong sustained cloud by the model, which further supports the presence of mixed-phase clouds at Jungfraujoch.

Whilst the inclusion of the surface crystal flux in Surf-3 provides a good comparison with the measured ice concentrations, the flux used is still a very simple parameterisation. Firstly, the surface crystal flux is independent of the surface concentration of surface hoar crystals. As the surface of the mountains upwind of Jungfraujoch will vary in distribution of surface hoar crystals present on the surface, the flux will vary dependent on the distribution of surface hoar crystals, in addition to the wind speed. The spatial and temporal variations of surface hoar suggested by Stossel et al. (2010) would need to be included in the parameterisation to better represent the surface crystal flux. Also, whilst the magnitude of the flux is calibrated based on our results, the surface crystal flux is adapted from an aerosol flux. To accurately assess the magnitude of the flux, measurements of surface crystal flux would be required to improve the physical understanding of the process of the advection of hoar crystals into the cloud.

Nonetheless, the results of the Surf-3 simulation suggest that the aerosol flux of Xu et al. (2013) can be adapted into a surface crystal flux and used in WRF. The inclusion of a surface crystal flux into WRF provides a good agreement between the simulated and measured ice number concentrations. In addition, the Surf-3 simulation suggests

ACPD
15, 25647–25694, 2015

that the inclusion of a surface crystal flux provides a good agreement with measured ice number concentrations without depleting the LWC, which is observed at Jungfraujoch, from the model. The presence of the LWC at Jungfraujoch in the Surf-3 simulation further suggests that the high ice concentrations in mixed-phase clouds observed at Jungfraujoch can be represented by including a flux of surface hoar crystals into the model. The simulation results support the suggestions of Lloyd et al. (2015), proposing that surface hoar crystals advected into cloud increases the ice concentration at Jungfraujoch.

5 Conclusions

In this paper, ice number concentrations from WRF model simulations were compared with ice number concentrations measured in orographic clouds Jungfraujoch during the INUPIAQ campaign. The ice number concentrations simulated in the model were significantly lower than the concentrations measured in-situ, which showed similarly high ice number concentrations to the concentrations witnessed in orographic clouds in previous field campaigns (Rogers and Vali, 1987; Targino et al., 2009). Suggestions for the high ice number concentrations witnessed in orographic clouds were explored using the model simulations.

Whilst increasing IN concentrations in the model produced a better representation of the observed ice number concentrations, the removal of liquid water from the model caused by the IN concentration suggested high IN concentrations would prevent the existence of the mixed-phase clouds witnessed at Jungfraujoch. Mixed-phase clouds are regularly witnessed at Jungfraujoch (Choularton et al., 2008; Lloyd et al., 2015), hence an accurate representation of LWC is required to understand the formation and influence of these orographic clouds. Our simulations suggest that whilst additional primary ice nucleation may contribute to ice concentrations in orographic clouds, increasing the IN concentration is not likely to be responsible for the high ice number concentrations observed.

ACPD
15, 25647–25694, 2015

Previous literature also suggested secondary ice production might contribute to an increased ice number concentration in orographic clouds. During the INUPIAQ campaign temperatures observed were outside the temperature range suggested by Hallett and Mossop (1974), implying ice multiplication was not responsible for increasing ice number concentrations. Following Targino et al. (2009), we analysed whether splinter production could occur close to cloud base and be blown into the cloud, and found using back trajectories that splinter concentrations only infrequently matched observed ice number concentrations. Whilst secondary ice production may be important in orographic clouds at warmer temperatures, secondary ice appears to have only a limited influence on the ice number concentrations observed during the INUPIAQ field campaign.

To evaluate if surface hoar crystals influence the ice concentrations in orographic clouds, a flux of hoar crystals from the surface was adapted from a frost flower aerosol flux and introduced into the WRF model. The inclusion of the flux provided a good agreement with the ice number concentrations measured at Jungfraujoch, suggesting the existence of such a flux may explain why surface measurements are higher than aircraft measurements of ice number concentration witnessed by Rogers and Vali (1987). The surface crystal flux parameterisation included in our simulations is a simple parameterisation, and independent of the surface concentration of surface hoar crystals. The spatial and temporal variations of surface hoar suggested by Stossel et al. (2010), such as varying hoar frost concentrations on the snow surface and the periods of hoar frost formation and removal, need to be included in the parameterisation to improve the accuracy of the surface flux. Nevertheless, the surface crystal flux parameterisation in this paper provides a good comparison with the observed ice number concentrations, and we suggest the increase in ice concentrations in orographic clouds is predominately influenced by a surface flux of hoar crystals.

Whilst aerosols acting as IN are important in initiating the production of ice in orographic clouds, they alone cannot explain the high ice number concentrations observed. There remains uncertainty on the exact causes of the high ice number concen-

ACPD
15, 25647–25694, 2015

trations in orographic clouds; however, we suggest the uncertainty may be accounted for by a flux of hoar crystals from the surface of the mountain. To verify the influence of a flux of surface hoar crystals on orographic clouds, observations and measurements of the flux are required. If the measurements confirm the effect, an improved representation of the flux can be provided using the new dataset and can be verified with the current field measurements.

Acknowledgements. The authors wish to express gratitude to colleagues from KIT, MPIC, PSI and University of Frankfurt who worked as part of CLACE 2014 for their support and assistance during the field campaign; to the staff at Jungfraujoch for access to their site and for their assistance and cooperation with our research. The lead author also wished to thank colleagues at the University of Manchester for their support and assistance. The INUPIAQ campaign is supported by a NERC standard grant award NE/K006002/1, whilst the lead author is supported by a NERC studentship and CASE funding from the UK Met Office. The data from this project can be obtained by contacting the authors of this article.

References

Albrecht, B. A.: Aerosols, cloud microphysics, and fractional cloudiness, Science, 245, 1227–1230, doi:10.1126/science.245.4923.1227, 1989. 25649

Alvarez-Aviles, L., Simpson, W. R., Douglas, T. A., Sturm, M., Perovich, D., and Domine, F.: Frost flower chemical composition during growth and its implications for aerosol production and bromine activation, J. Geophys. Res.-Atmos., 113, 1–10, doi:10.1029/2008JD010277, 2008. 25666

Ansmann, A., Tesche, M., Althausen, D., Müller, D., Seifert, P., Freudenthaler, V., Heese, B., Wiegner, M., Pisani, G., Knippertz, P., and Dubovik, O.: Influence of Saharan dust on cloud glaciation in southern Morocco during the Saharan Mineral Dust Experiment, J. Geophys. Res., 113, D04210, doi:10.1029/2007JD008785, 2008. 25649

Atkinson, J. D., Murray, B. J., Woodhouse, M. T., Whale, T. F., Baustian, K. J., Carslaw, K. S., Dobbie, S., O'Sullivan, D., Malkin, T. L., and O'Sullivan, D.: The importance of feldspar for ice nucleation by mineral dust in mixed-phase clouds, Nature, 498, 355–358, doi:10.1038/nature12278, 2013. 25650

ACPD

15, 25647–25694, 2015

Comparing Model and Measured Ice Crystal Concentrations

R. J. Farrington et al.

Title Page
Abstract | Introduction
Conclusions | References
Tables | Figures
◀ ▶
Back | Close
Full Screen / Esc
Printer-friendly Version
Interactive Discussion

Baltensperger, U., Gäggeler, H. W., Jost, D. T., Lugauer, M., Schwikowski, M., Weingartner, E., and Seibert, P.: Aerosol climatology at the high-alpine site Jungfraujoch, Switzerland, J. Geophys. Res., 102, 19707–19715, doi:10.1029/97JD00928, 1997. 25653

Baltensperger, U., Schwikowski, M., Jost, D. T., Nyeki, S., Gäggeler, H. W., and Poulida, O.: Scavenging of atmospheric constituents in mixed phase clouds at the high-alpine site Jungfraujoch part I: Basic concept and aerosol scavenging by clouds, Atmos. Environ., 32, 3975–3983, doi:10.1016/S1352-2310(98)00051-X, 1998. 25653

Barstad, I., Grabowski, W. W., and Smolarkiewicz, P. K.: Characteristics of large-scale orographic precipitation: evaluation of linear model in idealized problems, J. Hydrol., 340, 78–90, doi:10.1016/j.jhydrol.2007.04.005, 2007. 25652

Boucher, O., Randall, D., Artaxo, P., Bretherton, C., Feingold, G., Forster, P., Kerminen, V.-M., Kondo, Y., Liao, H., Lohmann, U., Rasch, P., Satheesh, S. K., Sherwood, S., Stevens, B., and Zhang, X. Y.: Clouds and aerosols, in: Climate Change 2013: The Physical Science Basis. Contribution of Working Group I to the Fifth Assessment Report of the Intergovernmental Panel on Climate Change, edited by: Stocker, T., Qin, D., Plattner, G.-K., Tignor, M., Allen, S., Boschung, J., Nauels, A., Xia, Y., Bex, V., and Midgley, P., Cambridge University Press, Cambridge, UK and New York, NY, USA, 571–657, doi:10.1017/CBO9781107415324.016, 2013. 25649

Broadley, S. L., Murray, B. J., Herbert, R. J., Atkinson, J. D., Dobbie, S., Malkin, T. L., Condliffe, E., and Neve, L.: Immersion mode heterogeneous ice nucleation by an illite rich powder representative of atmospheric mineral dust, Atmos. Chem. Phys., 12, 287–307, doi:10.5194/acp-12-287-2012, 2012. 25650

Cannon, D. J., Kirshbaum, D. J., and Gray, S. L.: A mixed-phase bulk orographic precipitation model with embedded convection, Q. J. Roy. Meteor. Soc., 140, 1997–2012, doi:10.1002/qj.2269, 2014. 25652

Chou, C., Stetzer, O., Weingartner, E., Jurányi, Z., Kanji, Z. A., and Lohmann, U.: Ice nuclei properties within a Saharan dust event at the Jungfraujoch in the Swiss Alps, Atmos. Chem. Phys., 11, 4725–4738, doi:10.5194/acp-11-4725-2011, 2011. 25655, 25658

Chou, M.-D. and Suarez, M. J.: A solar radiation parameterization for atmospheric studies, Tech. Rep. June, NASA/TM-1999-104606, 1999. 25656

Choularton, T. W., Bower, K., Weingartner, E., Crawford, I., Coe, H., Gallagher, M. W., Flynn, M., Crosier, J., Connolly, P., Targino, A., Alfarra, M. R., Baltensperger, U., Sjogren, S., Verheggen, B., Cozic, J., and Gysel, M.: The influence of small aerosol particles on the proper-

ties of water and ice clouds, Faraday Discuss., 137, 205–222, doi:10.1039/b702722m, 2008. 25653, 25659, 25669
Colbeck, S. C.: On the micrometeorology of surface hoar growth on snow in mountainous area, Bound.-Lay. Meteorol., 44, 1–12, doi:10.1007/BF00117290, 1988. 25665
Conen, F., Rodrìguez, S., Hüglin, C., Henne, S., Herrmann, E., Bukowiecki, N., and Alewell, C.: Atmospheric ice nuclei at the high-altitude observatory Jungfraujoch, Switzerland, Tellus B, 67, 1–10, 2015. 25655, 25658
Connolly, P. J., Flynn, M. J., Ulanowski, Z., Choularton, T. W., Gallagher, M. W., and Bower, K. N.: Calibration of the cloud particle imager probes using calibration beads and ice crystal analogs: the depth of field, J. Atmos. Ocean. Tech., 24, 1860–1879, doi:10.1175/JTECH2096.1, 2007. 25654
Connolly, P. J., Möhler, O., Field, P. R., Saathoff, H., Burgess, R., Choularton, T., and Gallagher, M.: Studies of heterogeneous freezing by three different desert dust samples, Atmos. Chem. Phys., 9, 2805–2824, doi:10.5194/acp-9-2805-2009, 2009. 25650
Conway, H. and Raymond, C. F.: Snow stability during rain, J. Glaciol., 39, 635–642, 1993. 25649
Cooper, W. A.: Ice initiation in natural clouds, Meteor. Mon., 21, 29–32, doi:10.1175/0065-9401-21.43.29, 1986. 25655, 25658, 25680
Crosier, J., Bower, K. N., Choularton, T. W., Westbrook, C. D., Connolly, P. J., Cui, Z. Q., Crawford, I. P., Capes, G. L., Coe, H., Dorsey, J. R., Williams, P. I., Illingworth, A. J., Gallagher, M. W., and Blyth, A. M.: Observations of ice multiplication in a weakly convective cell embedded in supercooled mid-level stratus, Atmos. Chem. Phys., 11, 257–273, doi:10.5194/acp-11-257-2011, 2011. 25650, 25654
Cziczo, D. J., Froyd, K. D., Hoose, C., Jensen, E. J., Diao, M., Zondlo, M. A., Smith, J. B., Twohy, C. H., and Murphy, D. M.: Clarifying the dominant sources and mechanisms of cirrus cloud formation, Science, 340, 1320–1324, doi:10.1126/science.1234145, 2013. 25649
de Boer, G., Morrison, H., Shupe, M. D., and Hildner, R.: Evidence of liquid dependent ice nucleation in high-latitude stratiform clouds from surface remote sensors, Geophys. Res. Lett., 38, L01803, doi:10.1029/2010GL046016, 2011. 25649
DeMott, P. J., Sassen, K., Poellot, M. R., Baumgardner, D., Rogers, D. C., Brooks, S. D., Prenni, A. J., and Kreidenweis, S. M.: African dust aerosols as atmospheric ice nuclei, Geophys. Res. Lett., 30, 1732, doi:10.1029/2003GL017410, 2003. 25649

ACPD
15, 25647–25694, 2015

Comparing Model and Measured Ice Crystal Concentrations

R. J. Farrington et al.

DeMott, P. J., Prenni, A. J., Liu, X., Kreidenweis, S. M., Petters, M. D., Twohy, C. H., Richardson, M. S., Eidhammer, T., and Rogers, D. C.: Predicting global atmospheric ice nuclei distributions and their impacts on climate, P. Natl. Acad. Sci. USA, 107, 11217–11222, doi:10.1073/pnas.0910818107, 2010. 25651

Domine, F., Taillandier, A. S., Simpson, W. R., and Severin, K.: Specific surface area, density and microstructure of frost flowers, Geophys. Res. Lett., 32, 1–4, doi:10.1029/2005GL023245, 2005. 25666

Emersic, C., J. Connolly, P., Boult, S., Campana, M., and Li, Z.: Investigating the discrepancy between wet-suspension and dry-dispersion derived ice nucleation efficiency of mineral particles, Atmos. Chem. Phys. Discuss., 15, 887–929, doi:10.5194/acpd-15-887-2015, 2015. 25650

Feick, S., Kronholm, K., and Schweizer, J.: Field observations on spatial variability of surface hoar at the basin scale, J. Geophys. Res., 112, 1–16, doi:10.1029/2006JF000587, 2007. 25666

Field, P. R., Heymsfield, A. J., Shipway, B. J., DeMott, P. J., Pratt, K. A., Rogers, D. C., Stith, J., and Prather, K. A.: Ice in clouds experiment–layer clouds. Part II: Testing characteristics of heterogeneous ice formation in lee wave clouds, J. Atmos. Sci., 69, 1066–1079, doi:10.1175/JAS-D-11-026.1, 2012. 25649

Galek, G., Sobik, M., Blaś, M., Polkowska, Z., Cichala-Kamrowska, K., and Walaszek, K.: Dew and hoarfrost frequency, formation efficiency and chemistry in Wroclaw, Poland, Atmos. Res., 151, 120–129, doi:10.1016/j.atmosres.2014.05.006, 2015. 25665

Galewsky, J. and Sobel, A.: Moist dynamics and orographic precipitation in Northern and Central California during the New Year's Flood of 1997, Mon. Weather Rev., 133, 1594–1612, doi:10.1175/MWR2943.1, 2005. 25649

Geever, M., O'Dowd, C. D., van Ekeren, S., Flanagan, R., Nilsson, E. D., de Leeuw, G., and Rannik, U.: Submicron sea spray fluxes, Geophys. Res. Lett., 32, 2–5, doi:10.1029/2005GL023081, 2005. 25667

Hachikubo, A. and Akitaya, E.: Effect of wind on surface hoar growth on snow, J. Geophys. Res., 102, 4367, doi:10.1029/96JD03456, 1997. 25665

Hallett, J. and Mossop, S. C.: Production of secondary ice particles during the riming process, Nature, 249, 26–28, doi:10.1038/249026a0, 1974. 25650, 25661, 25662, 25670

Harrington, J. Y., Meyers, M. P., Walko, R. L., and Cotton, W. R.: Parameterization of ice crystal conversion processes due to vapor deposition for mesoscale models using double-moment basis functions. Part I: Basic formulation and parcel model results, J. Atmos. Sci., 52, 4344–4366, doi:10.1175/1520-0469(1995)052<4344:POICCP>2.0.CO;2, 1995. 25664

Harris-Hobbs, R. L. and Cooper, W. A.: Field Evidence Supporting Quanitative Predictions of Secondary Ice Production, J. Atmos. Sci., 44, 1071–1082, doi:10.1175/1520-0469(1987)044<1071:FESQPO>2.0.CO;2, 1987. 25650

Helbig, N. and Van Herwijnen, A.: Modeling the spatial distribution of surface hoar in complex topography, Cold Reg. Sci. Technol., 82, 68–74, doi:10.1016/j.coldregions.2012.05.008, 2012. 25665

Hogan, R. J., Field, P. R., Illingworth, A. J., Cotton, R. J., and Choularton, T. W.: Properties of embedded convection in warm-frontal mixed-phase cloud from aircraft and polarimetric radar, Q. J. Roy. Meteor. Soc., 128, 451–476, doi:10.1256/003590002321042054, 2002. 25650

Hoose, C. and Möhler, O.: Heterogeneous ice nucleation on atmospheric aerosols: a review of results from laboratory experiments, Atmos. Chem. Phys., 12, 9817–9854, doi:10.5194/acp-12-9817-2012, 2012. 25650

Huang, Y., Blyth, A. M., Brown, P. R. A., Choularton, T. W., Connolly, P., Gadian, A. M., Jones, H., Latham, J., Cui, Z., and Carslaw, K.: The development of ice in a cumulus cloud over southwest England, New J. Phys., 10, 105021, doi:10.1088/1367-2630/10/10/105021, 2008. 25650

Koop, T., Luo, B., Tsias, A., and Peter, T.: Water activity as the determinant for homogeneous ice nucleation in aqueous solutions, Nature, 406, 611–614, doi:10.1038/35020537, 2000. 25649

Korolev, A. V. and Mazin, I. P.: Supersaturation of Water Vapor in Clouds, J. Atmos. Sci., 60, 2957–2974, doi:10.1175/1520-0469(2003)060<2957:SOWVIC>2.0.CO;2, 2003. 25659, 25687

Kunz, M. and Kottmeier, C.: Orographic enhancement of precipitation over low mountain ranges. Part II: Simulations of heavy precipitation events over southwest Germany, J. Appl. Meteorol. Clim., 45, 1041–1055, doi:10.1175/JAM2390.1, 2006. 25652

Lance, S., Brock, C. A., Rogers, D., and Gordon, J. A.: Water droplet calibration of the Cloud Droplet Probe (CDP) and in-flight performance in liquid, ice and mixed-phase clouds during ARCPAC, Atmos. Meas. Tech., 3, 1683–1706, doi:10.5194/amt-3-1683-2010, 2010. 25654

Lawson, R., Baker, B., Schmitt, C. G., and Jensen, T. L.: An overview of microphysical properties of Arctic clouds observed in May and July 1998 during FIRE ACE, J. Geophys. Res., 106, 14989–15014, 2001. 25654

Lawson, R. P., O'Connor, D., Zmarzly, P., Weaver, K., Baker, B., Mo, Q., and Jonsson, H.: The 2D-S (stereo) probe: design and preliminary tests of a new airborne, high-speed, high-resolution particle imaging probe, J. Atmos. Ocean. Tech., 23, 1462–1477, doi:10.1175/JTECH1927.1, 2006. 25654

Lawson, R. P., Woods, S., and Morrison, H.: The microphysics of ice and precipitation development in tropical cumulus clouds, J. Atmos. Sci., 72, 150310071420004, doi:10.1175/JAS-D-14-0274.1, 2015. 25650

Lloyd, G., Dearden, C., Choularton, T. W., Crosier, J., and Bower, K. N.: Observations of the origin and distribution of ice in cold, warm, and occluded frontal systems during the DIAMET campaign, Mon. Weather Rev., 142, 4230–4255, doi:10.1175/MWR-D-13-00396.1, 2014. 25650

Lloyd, G., Choularton, T. W., Bower, K. N., Gallagher, M. W., Connolly, P. J., Flynn, M., Farrington, R., Crosier, J., Schlenczek, O., Fugal, J., and Henneberger, J.: The origins of ice crystals measured in mixed phase clouds at High-Alpine site Jungfraujoch, Atmos. Chem. Phys. Discuss., 15, 18181–18224, doi:10.5194/acpd-15-18181-2015, 2015. 25651, 25652, 25653, 25654, 25657, 25658, 25659, 25661, 25665, 25669

Lohmann, U. and Feichter, J.: Global indirect aerosol effects: a review, Atmos. Chem. Phys., 5, 715–737, doi:10.5194/acp-5-715-2005, 2005. 25649

Lynn, B., Khain, A., Rosenfeld, D., and Woodley, W. L.: Effects of aerosols on precipitation from orographic clouds, J. Geophys. Res.-Atmos., 112, 1–13, doi:10.1029/2006JD007537, 2007. 25652

Mason, B. J.: The rapid glaciation of slightly supercooled cumulus clouds, Q. J. Roy. Meteor. Soc., 122, 357–365, doi:10.1256/smsqj.53002, 1996. 25650

Möhler, O., DeMott, P. J., Vali, G., and Levin, Z.: Microbiology and atmospheric processes: the role of biological particles in cloud physics, Biogeosciences, 4, 1059–1071, doi:10.5194/bg-4-1059-2007, 2007. 25650

Morrison, H., Curry, J. A., and Khvorostyanov, V. I.: A new double-moment microphysics parameterization for application in cloud and climate models. Part I: Description, J. Atmos. Sci., 62, 1665–1677, doi:10.1175/JAS3447.1, 2005. 25655, 25660

ACPD
15, 25647–25694, 2015

Comparing Model and Measured Ice Crystal Concentrations

R. J. Farrington et al.

Title Page
Abstract | Introduction
Conclusions | References
Tables | Figures
◀| |▶
◀ ▶
Back | Close
Full Screen / Esc
Printer-friendly Version
Interactive Discussion

Morrison, H., Thompson, G., and Tatarskii, V.: Impact of cloud microphysics on the development of trailing stratiform precipitation in a simulated squall line: comparison of one- and two-moment schemes, Mon. Weather Rev., 137, 991–1007, doi:10.1175/2008MWR2556.1, 2009. 25655

Mossop, S. C. and Hallett, J.: Ice crystal concentration in cumulus clouds: influence of the drop spectrum, Science, 186, 632–634, doi:10.1126/science.186.4164.632, 1974. 25650, 25662

Muhlbauer, A. and Lohmann, U.: Sensitivity studies of aerosol–cloud interactions in mixed-phase orographic precipitation, J. Atmos. Sci., 66, 2517–2538, doi:10.1175/2009JAS3001.1, 2009. 25652, 25655

Murray, B. J., Broadley, S. L., Wilson, T. W., Atkinson, J. D., and Wills, R. H.: Heterogeneous freezing of water droplets containing kaolinite particles, Atmos. Chem. Phys., 11, 4191–4207, doi:10.5194/acp-11-4191-2011, 2011. 25650

Na, B. and Webb, R. L.: A fundamental understanding of factors affecting frost nucleation, Int. J. Heat Mass Tran., 46, 3797–3808, doi:10.1016/S0017-9310(03)00194-7, 2003. 25665

Niemand, M., Möhler, O., Vogel, B., Vogel, H., Hoose, C., Connolly, P. J., Klein, H., Bingemer, H., DeMott, P. J., Skrotzki, J., and Leisner, T.: A particle-surface-area-based parameterization of immersion freezing on desert dust particles, J. Atmos. Sci., 69, 3077–3092, doi:10.1175/JAS-D-11-0249.1, 2012. 25650

Perovich, D. K. and Richter-Menge, J. A.: Surface characteristics of lead ice, J. Geophys. Res., 99, 16341–16350, doi:10.1029/94JC01194, 1994. 25666

Polkowska, Z., Sobik, M., Blas, M., Klimaszewska, K., Walna, B., and Namiesnik, J.: Hoarfrost and rime chemistry in Poland – an introductory analysis from meteorological perspective, J. Atmos. Chem., 62, 5–30, doi:10.1007/s10874-009-9141-6, 2009. 25665

Pratt, K. A., DeMott, P. J., French, J. R., Wang, Z., Westphal, D. L., Heymsfield, A. J., Twohy, C. H., Prenni, A. J., and Prather, K. A.: In situ detection of biological particles in cloud ice-crystals, Nat. Geosci., 2, 398–401, doi:10.1038/ngeo521, 2009. 25650

Prenni, A. J., Petters, M. D., Kreidenweis, S. M., Heald, C. L., Martin, S. T., Artaxo, P., Garland, R. M., Wollny, A. G., and Pöschl, U.: Relative roles of biogenic emissions and Saharan dust as ice nuclei in the Amazon basin, Nat. Geosci., 2, 402–405, doi:10.1038/ngeo517, 2009. 25650

Rankin, A. M. and Wolff, E. W.: A year-long record of size-segregated aerosol composition at Halley, Antarctica, J. Geophys. Res., 108, 1–12, doi:10.1029/2003JD003993, 2003. 25666

Rankin, A. M., Wolff, E. W., and Martin, S.: Frost flowers: implications for tropospheric chemistry and ice core interpretation, J. Geophys. Res.-Atmos., 107, 4683, doi:10.1029/2002JD002492, 2002. 25666

Rasmussen, R. M. R., Geresdi, I., Thompson, G., Manning, K., and Karplus, E.: Freezing drizzle formation in stably stratified layer clouds: the role of radiative cooling of cloud droplets, cloud condensation nuclei, and ice initiation, J. Atmos. Sci., 59, 837–860, doi:10.1175/1520-0469(2002)059<0837:FDFISS>2.0.CO;2, 2002. 25655

Roe, G. H.: Orographic precipitation, Annu. Rev. Earth Pl. Sc., 33, 645–671, doi:10.1146/annurev.earth.33.092203.122541, 2005. 25648

Rogers, D. C. and Vali, G.: Ice crystal production by mountain surfaces, J. Clim. Appl. Meteorol., 26, 1152–1168, doi:10.1175/1520-0450(1987)026<1152:ICPBMS>2.0.CO;2, 1987. 25651, 25657, 25661, 25665, 25668, 25669, 25670

Rotunno, R. and Houze, R. A.: Lessons on orographic precipitation from the Mesoscale Alpine Programme, Q. J. Roy. Meteor. Soc., 133, 811–830, doi:10.1002/qj.67, 2007. 25649

Sassen, K., DeMott, P. J., Prospero, J. M., and Poellot, M. R.: Saharan dust storms and indirect aerosol effects on clouds: CRYSTAL-FACE results, Geophys. Res. Lett., 30, 1633, doi:10.1029/2003GL017371, 2003. 25649

Schmitt, C. G. and Heymsfield, A. J.: Observational quantification of the separation of simple and complex atmospheric ice particles, Geophys. Res. Lett., 41, 1301–1307, doi:10.1002/2013GL058781, 2014. 25664

Shea, C. and Jamieson, B.: Spatial distribution of surface hoar crystals in sparse forests, Nat. Hazards Earth Syst. Sci., 10, 1317–1330, doi:10.5194/nhess-10-1317-2010, 2010. 25665

Skamarock, W. C., Klemp, J. B., Dudhia, J., Gill, D. O., Barker, D. M., Duda, M. G., Huang, X.-Y., Wang, W., and Powers, J. G.: A Description of the Advanced Research WRF Version 3, NCAR Technical Note, 2008. 25654

Stossel, F., Guala, M., Fierz, C., Manes, C., and Lehning, M.: Micrometeorological and morphological observations of surface hoar dynamics on a mountain snow cover, Water Resour. Res., 46, 1–11, doi:10.1029/2009WR008198, 2010. 25665, 25668, 25670

Style, R. W. and Worster, M. G.: Frost flower formation on sea ice and lake ice, Geophys. Res. Lett., 36, 20–23, doi:10.1029/2009GL037304, 2009. 25666

Targino, A. C., Coe, H., Cozic, J., Crosier, J., Crawford, I., Bower, K., Flynn, M., Gallagher, M., Allan, J., Verheggen, B., Weingartner, E., Baltensperger, U., and Choularton, T.: Influence of particle chemical composition on the phase of cold clouds at a high-alpine site in Switzerland,

ACPD
15, 25647–25694, 2015

J. Geophys. Res., 114, D18206, doi:10.1029/2008JD011365, 2009. 25651, 25653, 25658, 25659, 25661, 25669, 25670

Thompson, G., Rasmussen, R. M., and Manning, K.: Explicit forecasts of winter precipitation using an improved bulk microphysics scheme. Part I: Description and sensitivity analysis, Mon. Weather Rev., 132, 519–542, doi:10.1175/1520-0493(2004)132<0519:EFOWPU>2.0.CO;2, 2004. 25656

Twomey, S.: Pollution and the planetary albedo, Atmos. Environ., 8, 1251–1256, 1974. 25649

Vali, G.: Nucleation terminology, J. Aerosol Sci., 16, 575–576, doi:10.1016/0021-8502(85)90009-6, 1985. 25649

Vali, G., Leon, D., and Snider, J. R.: Ground-layer snow clouds, Q. J. Roy. Meteor. Soc., 138, 1507–1525, doi:10.1002/qj.1882, 2012. 25651

Verheggen, B., Cozic, J., Weingartner, E., Bower, K., Mertes, S., Connolly, P., Gallagher, M., Flynn, M., Choularton, T., and Baltensperger, U.: Aerosol partitioning between the interstitial and the condensed phase in mixed-phase clouds, J. Geophys. Res., 112, D23202, doi:10.1029/2007JD008714, 2007. 25653

Westbrook, C. D. and Illingworth, A. J.: Evidence that ice forms primarily in supercooled liquid clouds at temperatures $> -27\,^{\circ}$C, Geophys. Res. Lett., 38, L14808, doi:10.1029/2011GL048021, 2011. 25649

Westbrook, C. D. and Illingworth, A. J.: The formation of ice in a long-lived supercooled layer cloud, Q. J. Roy. Meteor. Soc., 139, 2209–2221, doi:10.1002/qj.2096, 2013. 25649

Xiao, H., Yin, Y., Jin, L., Chen, Q., and Chen, J.: Simulation of aerosol effects on orographic clouds and precipitation using WRF model with a detailed bin microphysics scheme, Atmos. Sci. Lett., 15, 134–139, doi:10.1002/asl2.480, 2014. 25652

Xu, L., Russell, L. M., Somerville, R. C. J., and Quinn, P. K.: Frost flower aerosol effects on Arctic wintertime longwave cloud radiative forcing, J. Geophys. Res.-Atmos., 118, 13282–13291, doi:10.1002/2013JD020554, 2013. 25666, 25667, 25668, 25680

Zubler, E. M., Lohmann, U., Lüthi, D., Schär, C., and Muhlbauer, A.: Statistical analysis of aerosol effects on simulated mixed-phase clouds and precipitation in the Alps, J. Atmos. Sci., 68, 1474–1492, doi:10.1175/2011JAS3632.1, 2011. 25652

ACPD
15, 25647–25694, 2015

Table 1. Summary of WRF simulations used in this paper.

Name	Details
Control	Control simulation
IN-1	Simulation with IN concentration increased by multiplying the Cooper equation (Cooper, 1986) by 10
IN-3	Simulation with IN concentration increased by multiplying the Cooper equation (Cooper, 1986) by 10^3
Surf-6	Simulation including a flux of surface crystals adapted from Xu et al. (2013), multiplied by $10^6\,m^{-2}\,s^{-1}$
Surf-3	Simulation including a flux of surface crystals adapted from Xu et al. (2013) multiplied by $10^3\,m^{-2}\,s^{-1}$

ACPD
15, 25647–25694, 2015

Table 2. Locations of Meteoswiss stations used to obtain Meteorological data throughout the INUPIAQ campaign.

Site	Latitude, °N	Longitude °E	Altitude, m	Model Altitude, m
Jungfraujoch	46.55	7.99	3580	3330
Eggishorn	46.43	8.09	2893	2320
Grimsel Hospiz	46.57	8.33	1980	2186
Titlis	46.77	8.43	3040	2337

ACPD
15, 25647–25694, 2015

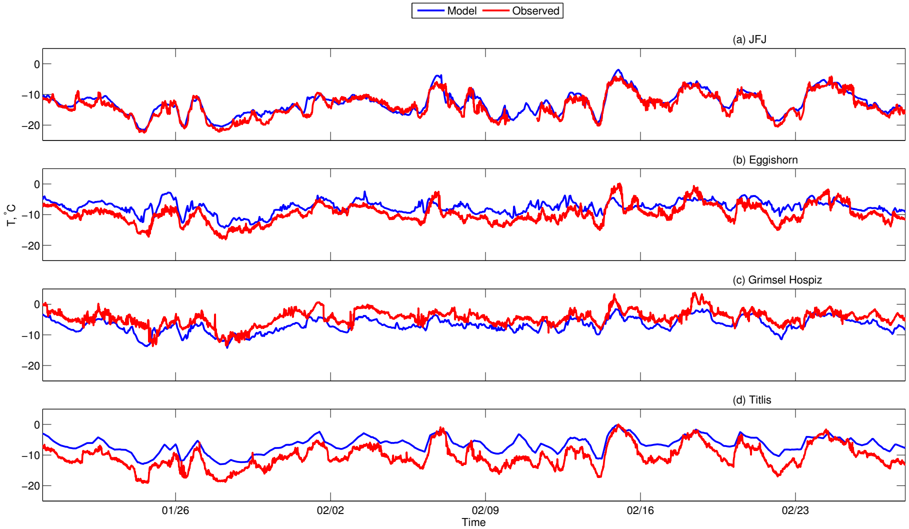

Figure 1. A comparison of the air temperature at 4 MeteoSwiss observation stations with the WRF control simulation during the INUPIAQ field campaign.

ACPD
15, 25647–25694, 2015

Comparing Model and Measured Ice Crystal Concentrations

R. J. Farrington et al.

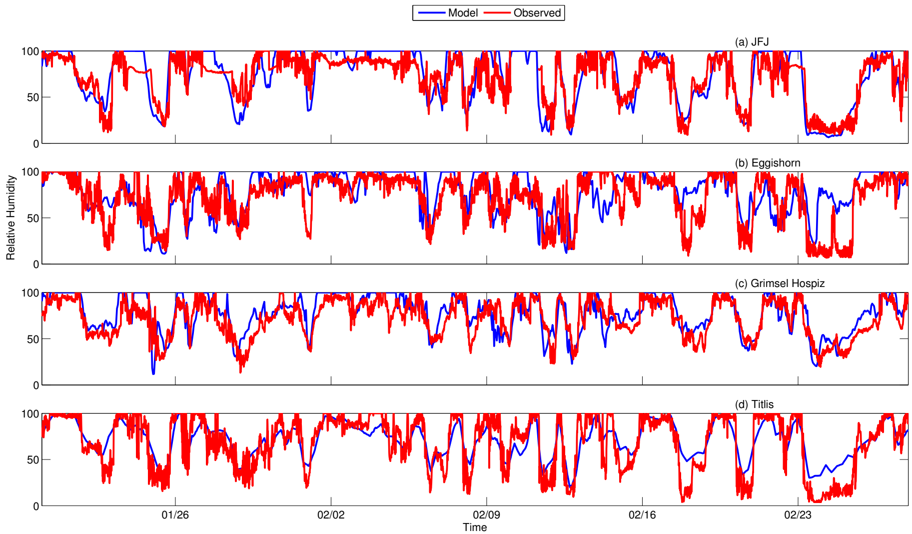

Figure 2. A comparison of the Relative Humidity at 4 MeteoSwiss observation stations with the WRF control simulation during the INUPIAQ field campaign.

ACPD
15, 25647–25694, 2015

Comparing Model and Measured Ice Crystal Concentrations

R. J. Farrington et al.

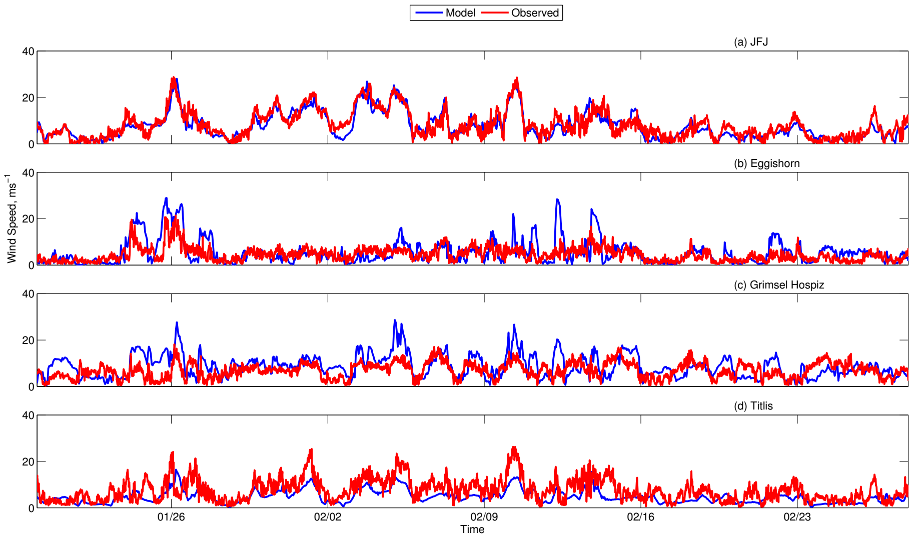

Figure 3. A comparison of the wind speed at 4 MeteoSwiss observation stations with the WRF control simulation during the INUPIAQ field campaign.

ACPD
15, 25647–25694, 2015

Comparing Model and Measured Ice Crystal Concentrations

R. J. Farrington et al.

ACPD
15, 25647–25694, 2015

Comparing Model and Measured Ice Crystal Concentrations

R. J. Farrington et al.

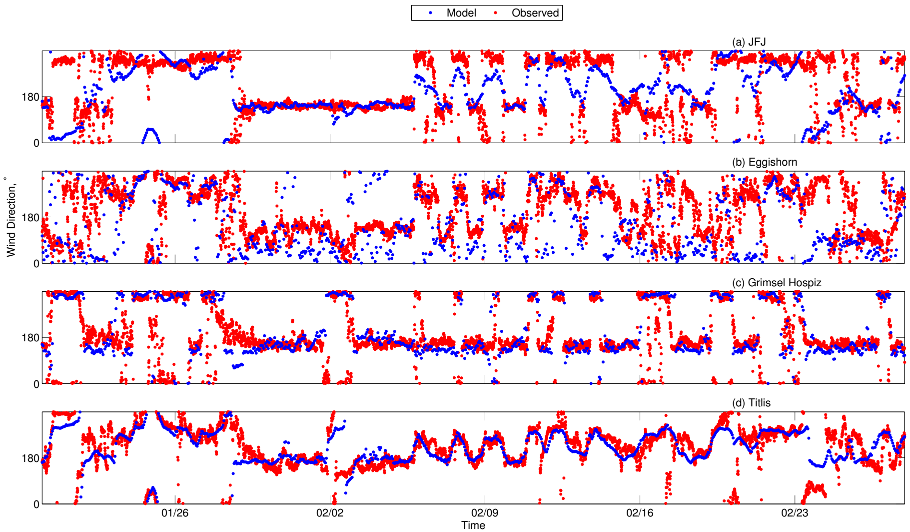

Figure 4. A comparison of the wind direction at 4 MeteoSwiss observation stations with the WRF control simulation during the INUPIAQ field campaign.

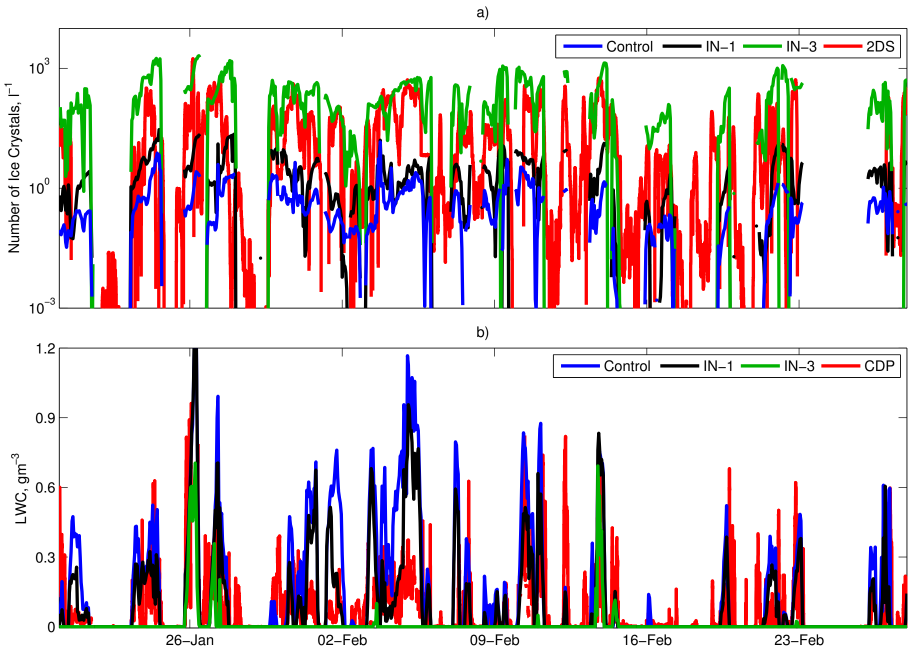

Figure 5. (a) Comparison of 2D-S ice number concentration measured at Jungfraujoch during the INUPIAQ campaign with the ice number concentration from the Control, IN-1 and IN-3 WRF model simulations. **(b)** Comparison of the CDP LWC measured at Jungfraujoch during the INUPIAQ campaign with the LWC from the Control, IN-1 and IN-3 WRF model simulations.

ACPD
15, 25647–25694, 2015

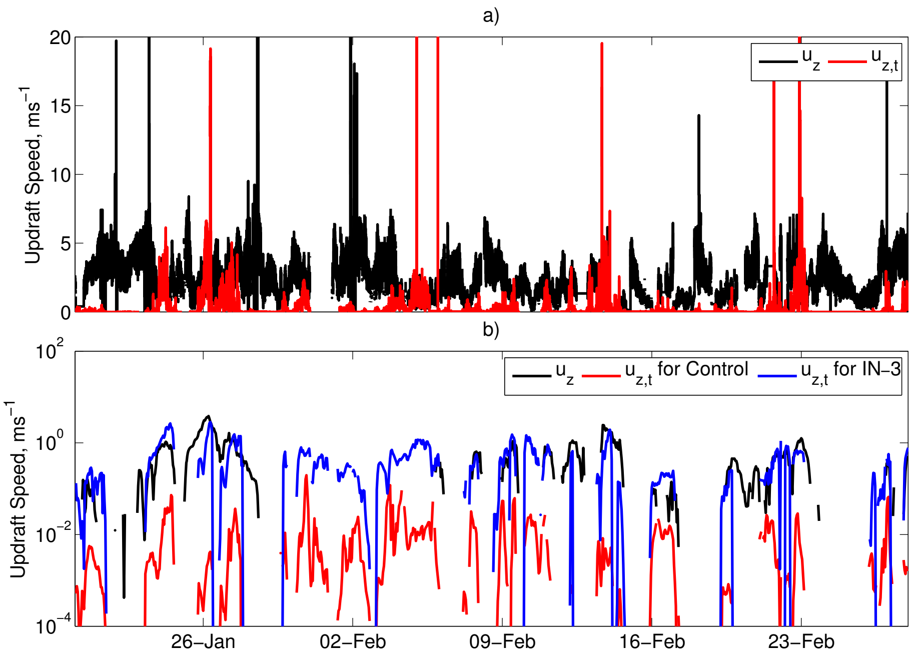

Figure 6. Analysis of updraft speed with the updraft threshold required for the presence of mixed-phase cloud, as defined by Eq. (2), which is adapted taken from Korolev and Mazin (2003). **(a)** compares the updraft speeds measured at Jungfraujoch (u_z) with the Korolev and Mazin (2003) updraft threshold (u_z) based on the 2D-S size distribution. **(b)** compares the simulated updraft speed at Jungfraujoch (u_z) with the updraft threshold calculated using the first moment of the ice size distributions ($u_{z,t}$) from the control and IN-3 WRF simulations.

ACPD
15, 25647–25694, 2015

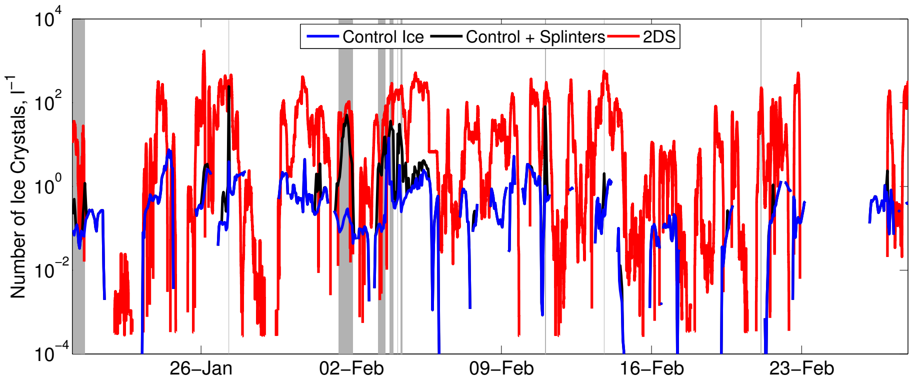

Figure 7. Comparison of ice number concentrations from the WRF control simulation, the control simulation with the addition of rime splinters produced by the Hallett–Mossop process calculated using Eq. (4), and the 2D-S probe at Jungfraujoch during the INUPIAQ Campaign. The grey shaded areas indicate periods where the ice number concentration including the splinters is at least a factor of 10 greater than the concentration from the WRF control simulation.

ACPD
15, 25647–25694, 2015

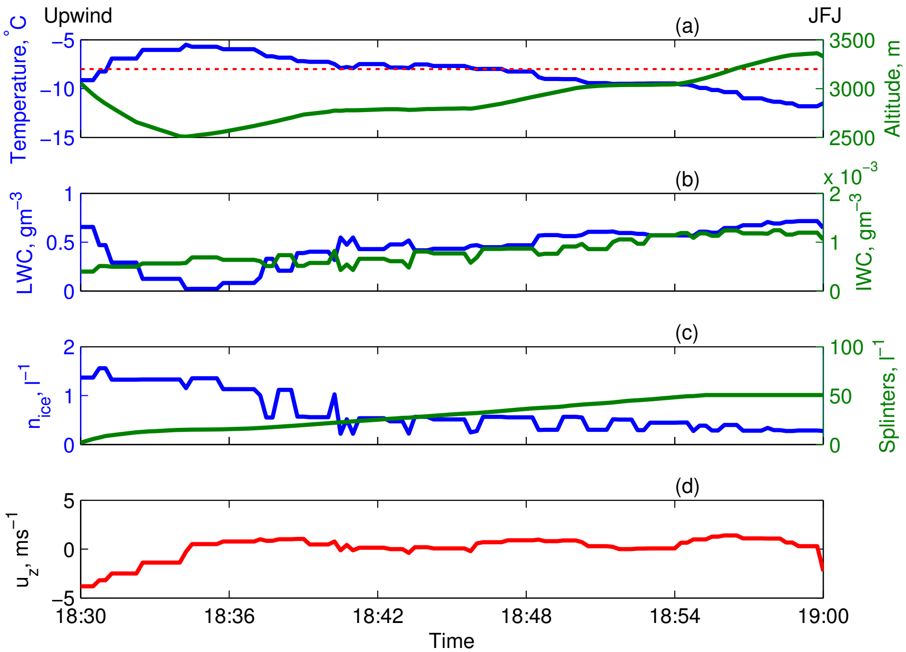

Figure 8. Variations in dynamical and microphysical properties along a back trajectory of air between a point upwind of the measurement site and Jungfraujoch itself on 1 February 2014, assuming a constant wind field. The constant wind field is taken from the WRF control simulation output of the 1 February 2014 at 19:00 Z. **(a)** Temperature and altitude along the back trajectory, with the red dashed line illustrating the −8 °C isotherm. **(b)** Liquid water content and ice water content along the back trajectory. **(c)** Ice number concentration from the WRF control run along the back trajectory, and the cumulative number of splinters produced along the trajectory, calculated using Eq. (4). **(d)** Vertical wind velocity along the back trajectory.

ACPD
15, 25647–25694, 2015

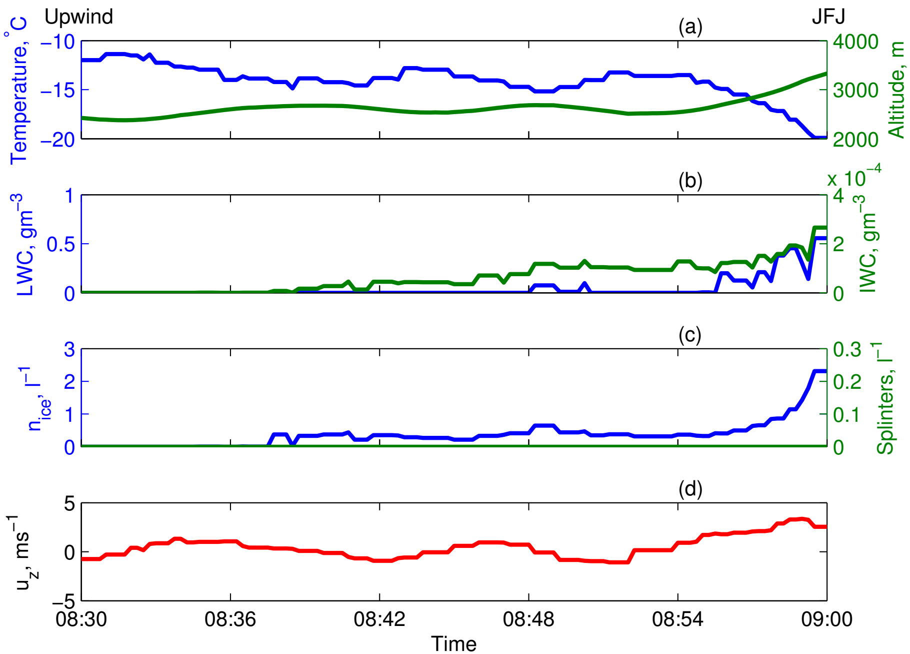

Figure 9. As for Fig. 8 but from the WRF simulation of 26 January 2014 at 09:00 Z.

ACPD
15, 25647–25694, 2015

Comparing Model and Measured Ice Crystal Concentrations

R. J. Farrington et al.

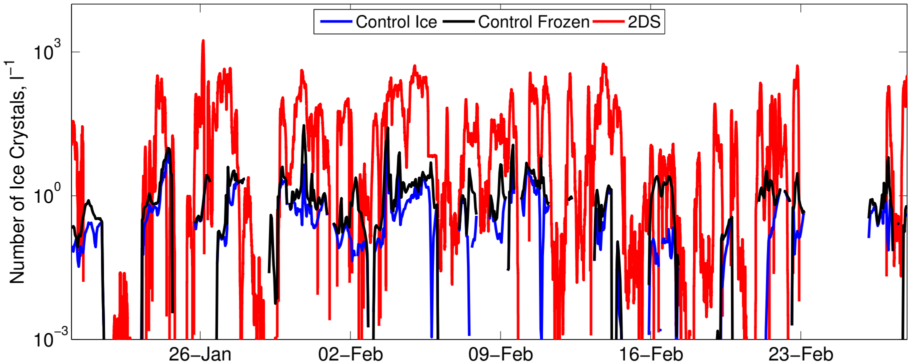

Figure 10. Comparison of measured 2D-S ice number concentration at Jungfraujoch during the INUPIAQ campaign with the ice concentration and the total frozen concentration measured by the control WRF model simulation at Jungfraujoch.

ACPD
15, 25647–25694, 2015

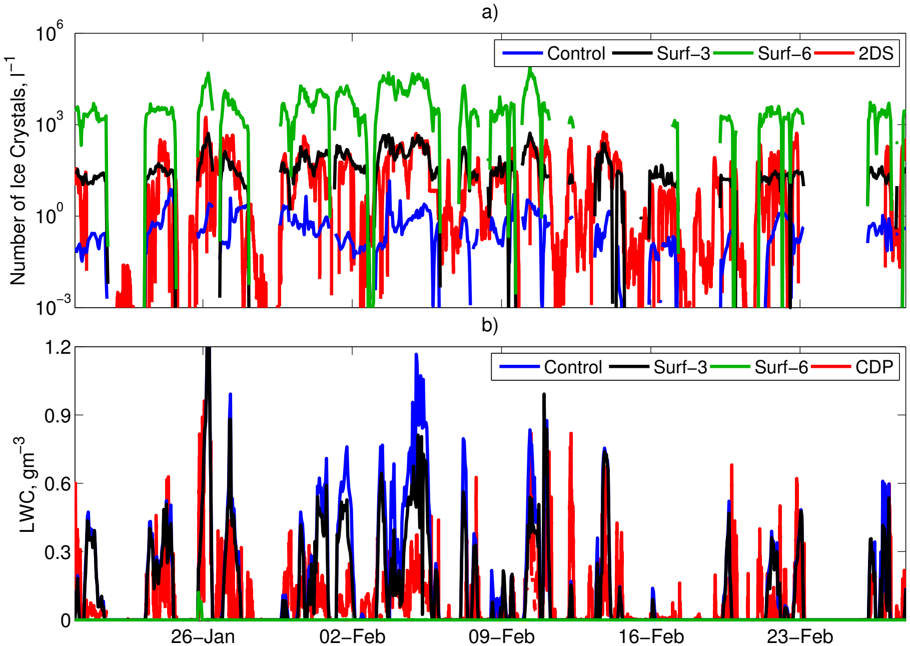

Figure 11. (a) Comparison of measured 2D-S ice number concentration at Jungfraujoch during the INUPIAQ campaign with the concentration from the control WRF model simulation, and the Surf-3 and Surf-6 simulations which included the addition of crystals from a surface flux calculated using Eq. (5). **(b)** Comparison of measured LWC at Jungfraujoch during the INUPIAQ Campaign with the LWC from the control WRF model simulation, and the Surf-3 and Surf-6 simulations, which included the addition of crystals from a surface flux. The black-dashed lines indicates the time-period of the cross sections plotted in Figs. 12 and 13.

ACPD
15, 25647–25694, 2015

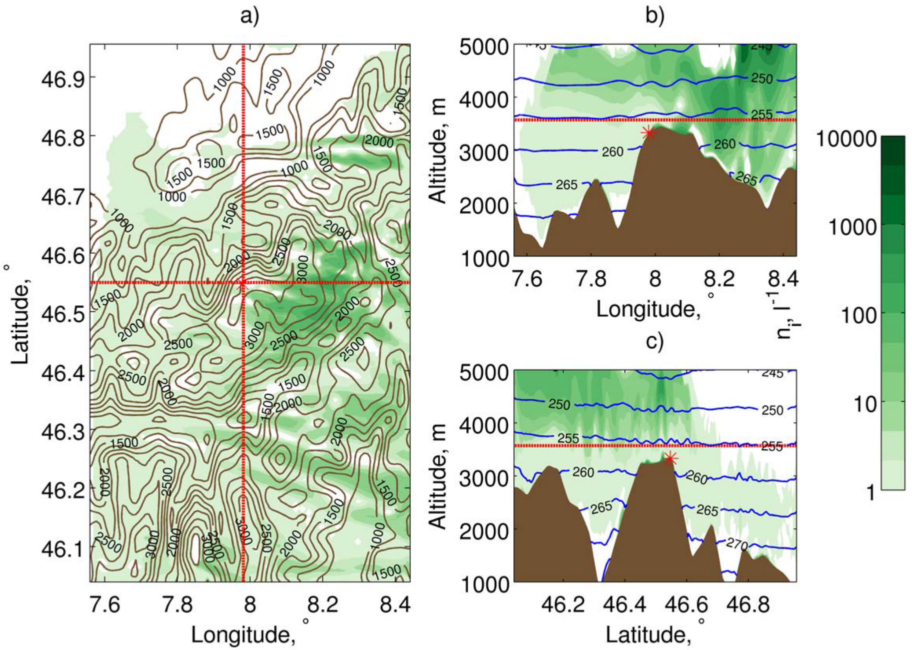

Figure 12. Ice number concentrations at 20:00 Z on 13 February 2014 from WRF model simulation including the addition of crystals from the surface crystal flux in 3 views. **(a)** represents a horizontal cross-section at the height of Jungfraujoch in reality (3570 m a.s.l.), with the red dashed lines representing the vertical cross-sections in **(b, c)**. **(b)** represents an east-west vertical cross-section at 46.55° Latitude, with red dashed line indicating the horizontal cross-section in **(a)**, and blue contours indicating isotherms in kelvin. **(c)** represents a north-south vertical cross-section at 7.98° Longitude, with red dashed line indicating the horizontal cross-section in **(a)**, and blue contours indicating isotherms in kelvin. In all 3 figures the location of Jungfraujoch is represented by the red star.

ACPD
15, 25647–25694, 2015

Comparing Model and Measured Ice Crystal Concentrations

R. J. Farrington et al.

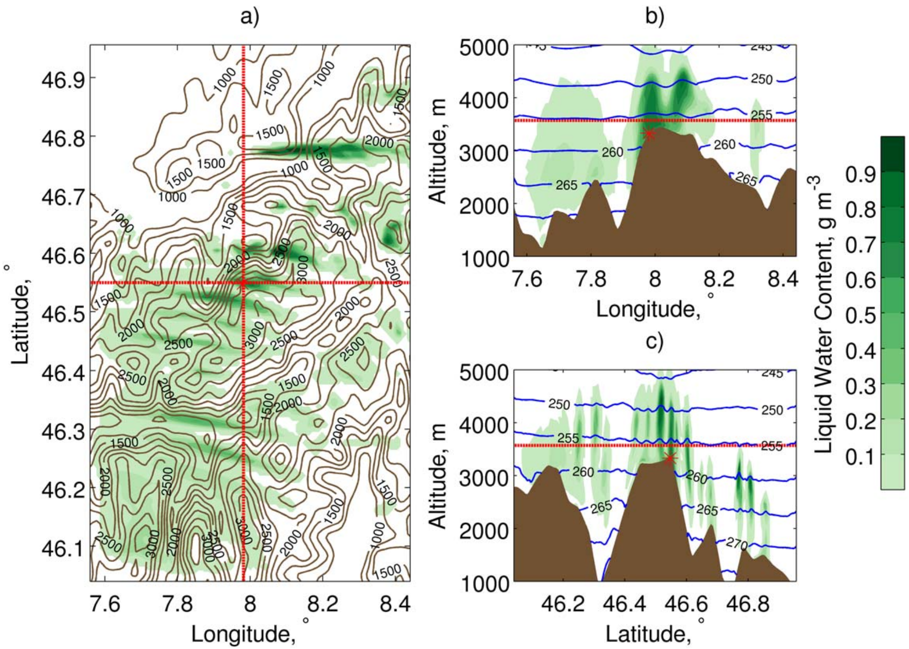

Figure 13. As Fig. 12 except for LWC at 20:00 Z on 13 February 2014.

ACPD
15, 25647–25694, 2015

Comparing Model and Measured Ice Crystal Concentrations

R. J. Farrington et al.

Title Page
Abstract Introduction
Conclusions References
Tables Figures
◀I ▶I
◀ ▶
Back Close
Full Screen / Esc
Printer-friendly Version
Interactive Discussion